Hindawi
Science and Technology of Nuclear Installations
Volume 2024, Article ID 9345812, 12 pages
https://doi.org/10.1155/2024/9345812

Research Article

Enhancing Resilience through Nuclear Emergency Preparedness at El Dabaa Site

Waad Saleh and Juyoul Kim

Department of NPP Engineering, KEPCO International Nuclear Graduate School, 658-91 Haemaji-ro, Seosaeng-myeon, Ulju-gun, Ulsan 45014, Republic of Korea

Correspondence should be addressed to Juyoul Kim; jykim@kings.ac.kr

Received 24 October 2023; Revised 24 January 2024; Accepted 27 January 2024; Published 13 February 2024

Academic Editor: Doddy Kastanya

The research utilized advanced PCTRAN and RASCAL software to evaluate the potential radiological impacts of hypothetical accidents, specifically loss-of-coolant accident (LOCA) and long-term station blackout (LTSBO), at the El Dabaa Nuclear Power Plant. Over a span of ten years, comprehensive meteorological data were meticulously analyzed to assess the dispersion of radioactive substances within a 40-kilometer radius across all four seasons. The outcomes revealed that only in the case of LTSBO did the radiological levels surpass the limits set by the Environmental Protection Agency (EPA). Notably, during spring, LTSBO exhibited a maximum total effective dose equivalent (TEDE) value of 13 millisieverts (mSv) at a distance of 3.2 kilometers, and the highest thyroid dose (TD) recorded was 63 mSv at 8 kilometers. These significant findings play a crucial role in shaping strategies related to the distribution of potassium iodide (KI) and further enhance the overall preparedness and evacuation planning protocols.

1. Introduction

The El Dabaa nuclear plant will be situated in Marsa Matrouh governorate, approximately 320 kilometers northwest of Cairo and west of Alexandria, Egypt. It comprises four VVER-1200 nuclear power units. The construction of the plant will be undertaken by Rosatom's subsidiary company, in collaboration with the Korea Hydro and Nuclear Power (KHNP) [1]. During normal operation, reactors release minimal radionuclides [2, 3]. However, severe accidents involving core meltdown or surpassing design limits can result in substantial radionuclide release [2, 3]. After a significant accident, radionuclides can pose risks to plant staff, public health, and the environment [4]. The extent of radionuclide release and the seriousness of the event that caused it determine how serious the threat is [3, 5]. Given the potentially lethal nature of nuclear radiation, assessing potential radiological hazards resulting from catastrophic accidents is essential [6]. This evaluation should consider the vulnerability of the plant's safety mechanisms [3]. Past incidents at Three Mile Island, Chernobyl, and Fukushima Daiichi have shown how nuclear accidents can lead to extensive radioactive pollution locally, regionally, and globally [5]. Consequently, when considering the establishment of a new nuclear facility, the significance of developing emergency readiness programs becomes imperative [6]. Ensuring readiness requires vital details such as site locations, plume arrival times at key spots, and background radiation levels. This level of preparedness relies on sophisticated tools such as dispersion models and detailed meteorological databases, encompassing wind speed and direction for precise forecasting [5]. Simulation emerges as an indispensable tool for providing early decision support in emergency scenarios, facilitating the evaluation of accident consequences [5]. Diverse software tools are leveraged to assess the impact of radiological and nuclear incidents, with a specific emphasis on atmospheric dispersion modeling. Prominent examples encompass MLDP (Modèle Lagrangien de Dispersion de Particules d'ordre), NAME (Numerical Atmospheric-dispersion Modeling Environment), RATM

(Regional Atmospheric Transport Model), FLEXPART (Flexible Particle Dispersion Model), SPEEDI (System for Prediction of Environmental Emergency Dose Information), WSPEEDI (Worldwide SPEEDI), RIMPUFF (Risø Mesoscale PUFF model), ADMS (Atmospheric Dispersion Modeling System), JRODOS (Java-based Real-time Online Decision Support), HYSPLIT (Hybrid Single-Particle Lagrangian Integrated Trajectory), HotSpot (Gaussian Plume Model), RASCAL (Radiological Assessment System for Consequence Analysis), PC CREAM (Consequences of Releases to the Environment Assessment Methodology), and others. These tools collectively contribute to a comprehensive understanding of atmospheric transport and dispersion, which are crucial factors in predicting the radiological impact during potential nuclear emergencies [7–9]. Gaussian plume models remain extensively employed for risk assessment and emergency responses. These models find application in various software, including "Radiological Assessment System for Consequence Analysis," RASCAL [10, 11]. PCTRAN, short for "Personal Transient Computer Analyzer," simulates nuclear power plant transients and accidents on personal computers. Its user-friendly graphical interface enables direct interaction with simulation elements. It is an easy operation, faster-than-real-time execution and suitable for various plant types, and is recognized by the International Atomic Energy Agency (IAEA) [12, 13].

As Egypt's nuclear involvement poses significant challenges, demanding strong emergency strategies at local and national levels [14, 15]. The aim of this study is to enhance strategies for public safety and environmental protection as well as improve emergency response planning and decision-making by integrating PCTRAN-modeled transient and accident sequences, encompassing both design basis accidents (DBA) and beyond design basis accidents (BDBA), into RASCAL.

2. Literature Review of Previous Studies

Nuclear power plants are commonly viewed as environmentally friendly energy sources with a minimal carbon footprint, making them a promising solution to the escalating global energy demand [16]. Nevertheless, the apprehension of a significant or severe accident occurring in a nuclear power plant has, to some extent, impeded the growth and development of this industry among the general population [17]. The Fukushima Daiichi nuclear accident in 2011 underscored the susceptibility of nuclear facilities to natural disasters, particularly when lacking essential safety features. The extensive release of radioactive materials into seawater and soil following this incident triggered significant concerns among researchers [18, 19]. This paper conducted a thorough examination of the Fukushima accident, focusing on the release and dispersion of radioactivity in the environment. It delves into the repercussions on public health, the economy, energy policies, international relations, and the development of light water reactor (LWR) fuel [20]. This paper outlined the variations in safety preparations at Chernobyl and Fukushima Daiichi, providing recommendations for enhancing safety culture, decontamination practices, and disaster planning. Additionally, it addressed the necessity for implementing a high-level national emergency response system to effectively manage nuclear accidents [21]. In this paper, showcase outcomes derived from the efficient RASCAL 4.2 code applied to the Fukushima Daiichi accident are presented. By leveraging comparable Nuclear Power Plants (NPPs) already cataloged in the RASCAL database of U.S. NPPs and incorporating tailored accident event sequences for each unit at Fukushima, the released Source Term into the atmosphere is assessed [22].

In a series of PCTRAN-based studies, Omar and Hasan [23] conducted a comparative loss of coolant accident (LOCA) analysis, investigating severity in the VVER 1200 plant's hot and cold legs. The study explored break size impact, simulating various scenarios, including station blackout (SBO) and emergency core cooling system (ECCS) malfunction. Similarly, Fyza et al. [24] used PCTRAN to analyze thermal-hydraulic parameters of the VVER-1200 plant during a LOCA with offsite power loss. Additionally, Akter et al. [25] used PCTRAN for a reactor transient simulation, focusing on turbine trips and anticipated transient without scram (ATWS) events in AP-1000 and VVER-1200 reactors. Furthermore, Tanim et al. [26] conducted a fault consequences analysis using PCTRAN. The study explored various faults, including feedwater loss, steam generator tube rupture (SGTR), and coolant break. Factors such as reactivity, steam/feedwater flow, pressure, and more were analyzed through transient behavior analysis.

In the realm of RASCAL studies, Bakr [15] used probabilistic safety assessment (PSA) to establish emergency zones for the El-Dabaa NPP. A severe accident scenario for the VVER-1200 reactor was simulated, considering varied atmospheric patterns and probabilities. Additionally, Abd El-Hameed and Kim [27] utilized the RASCAL code to analyze radioactive material release from the VVER-1200 reactor in diverse scenarios. Output data were utilized in a machine learning classification and regression tree (CART) model to predict material quantities based on specific parameters at the El Dabaa site. Moreover, Khai and Cuong [28] used RASCAL to evaluate radiation doses resulting from radioactive release at Ninh Thuan 1 NPP. Their focus was on INES-level 7 nuclear accidents, encompassing scenarios involving station blackout (SBO) and loss of LOCA incidents. Furthermore, Faisal et al. [29] investigated a VVER-1200 reactor's station blackout (SBO) incident using RASCAL. Lastly, Shiuli et al. [30] undertook a VVER-1200 radiological safety analysis using RASCAL and HOTSPOT codes. They examined reactor accidents at different international nuclear event scale (INES) levels (5, 6, and 7) due to SBO and loss of LOCA incidents, analyzing emergency response at the Rooppur site during both dry and rainy seasons. In contrast to previous RASCAL studies where accident sequence scenarios were either assumed by authors or simulated using general pressurizer water reactor (PWR) descriptions, this study takes a distinct approach. The accident scenario transients will be implemented by directly using the transient responses of VVER-1200 reactor systems using PCTRAN. This approach aims to offer a more precise and specific representation of accident situations.

3. Methodology

In this study, the methodology includes four procedures, as illustrated in Figure 1.

(1) The first procedure involves meteorological data analysis, where a 10-year dataset of meteorological information was gathered and organized into categories corresponding to the four distinct seasons.

(2) The second procedure involves the analysis of accident scenario event sequences. This step utilizes the PCTRAN-VVER 1200 data as input into the RASCAL software to simulate LOCA with and without emergency core cooling system (ECCS) and LTSBO.

(3) The third procedure encompasses calculation of source term and corresponding doses.

(4) The fourth procedure is the radiological assessment to evaluate potential impacts, by comparing dose results against established guidelines to determine appropriate actions.

3.1. Weather Data. A detailed examination was carried out on temperature, wind speed, precipitation, stability classification, and wind direction data spanning a ten-year period. Quartiles and median values were employed since the data deviated from a normal distribution, helping to capture representative values for each condition. The outcomes of this analysis are presented in Table 1.

3.2. Simulation Models

3.2.1. RASCAL. The latest version of the "Radiological Assessment System for Consequence Analysis," known as RASCAL 4.3.4, is a specialized tool developed by the U.S. NRC's Protective Measures Team to assess the impact of radioactive accidents. This comprehensive system comprises seven distinct tools, with a focus on consequence assessment. Notably, the four core tools include Source Term to Dose (STDose), Field Measurement to Dose (FMDose), Radionuclide Data Viewer, and Decay Calculator. Among these, STDose and FMDose are pivotal for independent radiation dose predictions, aiding in decision-making during nuclear incidents. RASCAL 4.3.4 employs the STDose model, a key component, to estimate radiation exposure downstream. This involves diverse dose pathways such as inhalation, ground shine, and cloud shine. Equation (1) in RASCAL represents the fundamental Gaussian puff model, applying the superposition principle to extend the one-dimensional solution of the diffusion equation to three dimensions. This mathematical approach forms the basis for modeling the dispersion of radioactive materials and calculating radiation doses in the affected areas.

$$\frac{X(x,y,z)}{Q} = \frac{1}{(2\pi)^{3/2}\sigma_x\sigma_y\sigma_z}\exp\left[-\frac{1}{2}\left(\frac{x-x_0}{\sigma_x}\right)^2\right] \times \exp\left[-\frac{1}{2}\left(\frac{y-y_0}{\sigma_y}\right)^2\right] \times \exp\left[-\frac{1}{2}\left(\frac{z-z_0}{\sigma_z}\right)^2\right], \quad (1)$$

where Q is the amount of unconfined radioactive material released during the accident, measured in becquerels (Bq) or grams (g). σ is the dispersion parameter, which depends on the distance from the release point. It is used in conjunction with a transport device to pass through the puff's centre (x_0, y_0, and z_0). The dispersion parameter is measured in meters (m). χ is the concentration of the radioactive material in the atmosphere, measured in becquerels per cubic meter (Bq/m^3) or grams per cubic meter (g/m^3). This represents the amount of radioactive material present in the air at a specific location and time.

As the transport model exclusively calculates air concentration and ground surface concentration for a unit release, it becomes necessary to adjust these values for each radionuclide using the dose model. Radiologic decay leads to the depletion of each radionuclide in the source term over the assessment period. The outcome is then multiplied by the cumulative air concentration calculated for a unit release, considering whether the material is depositing or non-depositing, as appropriate for that particular radionuclide [31]. The early phase TEDE, as outlined by the Environmental Protection Agency (EPA), encompasses cloudshine dose, inhalation CEDE, and the groundshine dose accumulated within the initial 96 hours following the commencement of the release into the environment. The Thyroid Committed Dose Equivalent represents a 50-year committed dose to an adult man, encompassing contributions from all radionuclides. These dose equivalents are calculated by summing over all radionuclides of the products of the exposure to each radionuclide during the 15-minute period, the radionuclide and organ-specific dose conversion factor, and the breathing rate [10, 32]. In the early phase, doses can be derived by either using the average air concentration during the radioactive plume's passage or ground concentration immediately after its transit. This assumes measurement accuracy for plume radiation and considers exposure to both plume and surface radiation over the plume's passage and the following 96 hours. The method assumes constant plume concentration during passage. This forms the basis for estimating early-phase incident doses. The main aim is to evaluate whether radionuclide concentrations could lead to doses exceeding Protective Action Guides (PAGs) set by the U.S. Environment Protection Agency (EPA) which appropriate protective actions [10, 33].

3.2.2. PCTRAN. This study utilized PCTRAN-VVER1200, a specialized Nuclear Transient Accident Simulator developed by Micro Simulation Technology. PCTRAN, an acronym for "Personal Transient Computer Analyzer," is a PC-based program designed for simulating transient events and accidents across various reactor models, such as PWR, BWR, advanced AREVA EPR, Westinghouse AP1000, and GE ABWR [2]. PCTRAN has been effectively utilized by the IAEA as a training platform. Its adaptability and wide applicability make it invaluable for nuclear power safety analysis and training [34]. Past PCTRAN studies primarily focused on simulating fault scenarios within a VVER-1200 reactor, investigating their effects on key parameters

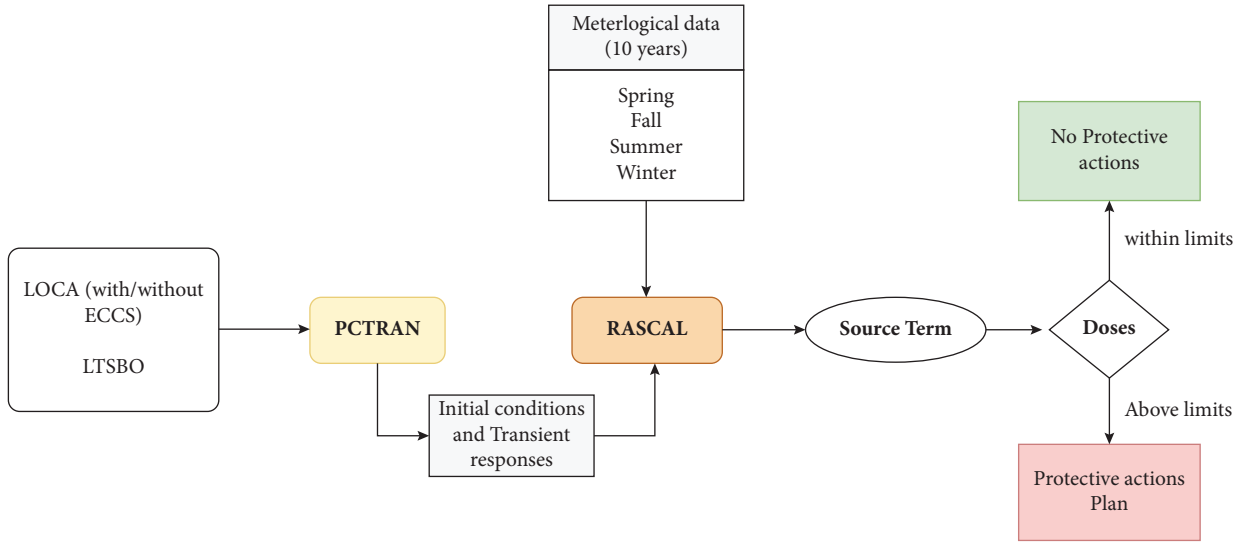

Figure 1: Flowchart for the study procedures.

Table 1: Weather data for El Dabaa site.

Factors	Season	Fall	Spring	Summer	Winter
Temperature (°C)	1st Q	16.4	21.4	24.8	12.2
	Median	19.2	24.2	26.8	15.1
	3rd Q	22.2	26.6	29.2	17.8
Wind speed (m/s)	1st Q	2			
	Median	3			
	3rd Q	4			
Wind direction predominant range		332.5–337.5	312.5–317.5		247.5–252.5
Predominant stability class		D			
		C			
		E			

including reactivity, steam and feedwater flow, and pressure. This current study takes a step further by examining the radiological consequences of these scenarios, extending the analysis to environmental radiation protection considerations. The transient sequence in the PCTRAN file is cross-referenced with prior research about LOCA without ECCS, the timing of events in this study is compared with a 2800 m^2 large break LOCA from [23], revealing only minor differences in timing, measured in seconds. For instance, in the referenced study, core exposure takes place after 27.5 seconds, whereas in this study, with a slightly larger 3000 m^2 break, core exposure occurs in just 25 seconds. This validation process for some of study's scenarios confirms the accuracy of the transient behavior analysis by aligning it with these comparative studies. However, the core inventory (source-term) is evaluated by integrating the transient responses of reactor systems from PCTRAN into the RASCAL software. The analysis covered three accident scenarios at El Dabaa NPP.

3.3. Hypothetical Accident Scenarios. This study involves the simulation of diverse accident scenarios, encompassing Beyond Design Basis Accidents (BDBA) along with Design Basis Accident (DBA) at EL Dabaa NPP Unit-1. These simulations replicate events modeled in PCTRAN and integrate them into the RASCAL software. The study follows predefined accident sequences and malfunctions, aiming to explore the radiological consequences associated with these scenarios [34, 35].

3.3.1. Scenario-1 (S1). In this scenario, a cold leg undergoes a significant large break, leading to a sizable 3000 cm^2 opening for the discharge of reactor coolant. The ECCS remains operational, without any error for activation.

3.3.2. Scenario-2 (S2). In this scenario, a Large Break Loss of Coolant Accident (LBLOCA) is simulated in a cold leg. Unlike the previous scenario S1, ECCS functionality is not considered in this case.

3.3.3. Scenario-3 (S3). In this scenario, a LTSBO is simulated, resulting in a total loss of alternating current (AC) power. Additionally, it is assumed that the turbine-driven auxiliary feedwater pump is not available.

The VVER-1200, which stands for "Water-Water Energetic Reactor 1200," belongs to the category of Generation-III + pressurized water type nuclear reactors. Table 2 shows

Table 2: Technical specifications of the VVER-1200 reactor for simulation.

Parameter	Initial condition input data	
	RASCAL	PCTRAN
Type	Generic PWR with large, dry containment	VVER-1200
Reactor power	3200 MWth [36, 37]	
Average burnup-in reactor	40000 MWd/MTU [36, 37]	
Discharge burnup-in spent fuel storage	50000 MWd/MTU [36, 37]	
Number of assemblies in core	163 [36, 37]	
Containment volume	$2.5E+06\,ft^3$ [28]	
Volume RCS liquid	$345.3\,m^3$ (VOL from transient file)	
U tubes inside each steam generator (SG)	10978 [36, 37]	
SG water inventory	64999.8 kg (MSGA from transient file)	
Steam flow rate SG A	$1.0E+06$ kg/hr (maximum value into rascal)	$1.57E+06$ kg/hr

the VVER-1200 reactor's technical parameters for simulation. It features enhanced safety measures compared to earlier models. The reactor is designed with five levels of engineering safety barriers aimed at preventing the release of radiation into the environment. Notably, the VVER-1200 incorporates advanced passive safety mechanisms capable of functioning during prolonged SBO events or interruptions in cooling water supply to the reactor core. These passive safety systems can operate for approximately 72 hours during an SBO scenario. In case of a severe accident, a contemporary core catcher is used to contain molten materials, effectively preventing contamination of soil, water, or the environment. This design substantially reduces the likelihood of environmental impact resulting from both design and beyond design basis accidents in this type of nuclear power plant [38]. Nonetheless, it remains essential to conduct pre-estimations of potential risks associated with accidents in nuclear power plants. Such assessments are crucial in ensuring preparedness for nuclear and radiological emergencies, while also safeguarding the well-being of workers and public from potential health hazards. Table 3 shows all simulated accident scenarios' event sequences. Applying all the transients from PCTRAN into RASCAL presented certain limitations. As indicated in Table 3, radionuclide emissions from the reactor core initiate after an 8-hour interval, corresponding with the default delay duration of 8 hours (default value) for LTSBO as set by the SOARCA RASCAL study [10]. Also, the maximum value can be simulated for steam flow rate into RASCAL is $1.0E+06$ kg/hr. Furthermore, another limitation concerns the timing of core exposure during LTSBO, a scenario not encountered in transients modeled by PCTRAN. In Figure 2, the core remaining covered throughout the simulation for 15 hr and the diesel generator starting automatically (D/G A) after a 60.0-second delay (postreactor scram within 26 sec). Additionally, the high-pressure safety injection system and spray system activate only after 3.5 hours.

4. Results and Discussion

4.1. Source Term Investigation. The study source term is divided into eight groups, selected from prior literature with a primary focus on VVER 1000 and VVER 1200 [3, 39]. These groups include noble gases, halogens, alkali metals, tellurium group, Ba/Sr group, noble metals, cerium group, and lanthanides. Figure 3 displays the source term groups' activity in Becquerel (Bq) for all scenarios. The contribution of radionuclides to the source term is influenced by several significant factors, including fission product yield, the nuclide's physical state, chemical activity, its reaction to reduction mechanisms, and most importantly, the severity of the accident [3]. As shown in Figure 3, the dominant contributors to the source term are noble gases and halogens, constituting total activity $5.1E+17$ Bq and $7.1E+15$ Bq, respectively. The contributions from other groups are $4.8E+15$ Bq for all scenarios. In a previous study [29], using RASCAL for LTSBO, the activities of certain radionuclides from different groups, such as I-131, Cs-137, Mo-99, and Sr-90, were reported as $2.3E+15$ Bq, $2.8E+14$ Bq, $9.6E+14$ Bq, and $1.1E+12$ Bq, respectively. In the present study, the corresponding activity levels for these radionuclides are $1.5E+15$ Bq, $2.0E+14$ Bq, $6.4E+14$ Bq, and $7.8E+11$ Bq, respectively. This divergence arises from the different initial conditions including average burn up, primary coolant mass, and steam generator water mass in addition the availability of the spray system. In a prior study by Shiuli et al. [30], which considered LOCA concurrent with SBO, the activity of I-131 was noted as $1.6E+15$ Bq, and for Cs-137, it was $2.6E+15$ Bq. Conversely, for the LOCA scenario without ECCS in this current study, the activities were found to be lower at $3.1E+13$ Bq for I-131 and $4.0E+12$ Bq for Cs-137. This disparity in activity levels between the two scenarios can be attributed to the differing accident severities, with Shiuli et al's study [30] indicating a more severe accident due to the absence of AC power.

4.2. Dose Assessment

4.2.1. Total Effective Dose Equivalent. The maximum dose values in millisieverts (mSv) were calculated within a 25-mile radius (40.2 km) from the nuclear plant. The data were presented graphically in Figure 4, where (a), (b), and (c) represented scenarios S1, S2, and S3, respectively. These scenarios were tested under different weather conditions outlined in Table 1. In each graph, it was observed that the most intense radiation exposure occurred at a distance of about 0.4 km from the release point. As the distance increased beyond this point, radiation exposure gradually decreased. In case of LOCA with ECCS

Table 3: Sequences of events within accident scenarios.

Type of accident	LOCA S1	LOCA S2	LTSBO S3
Shutdown	Mm 06 : 00 (month is depending on seasons timing)		
Simulation period	96 hours		
Release start (core uncovered)	After 25 second	After 25 second	After 8 hr in rascal (default value)
Core status	Recovered after 3735 second	Vessel meltdown	Core recovered in rascal after 3 hr

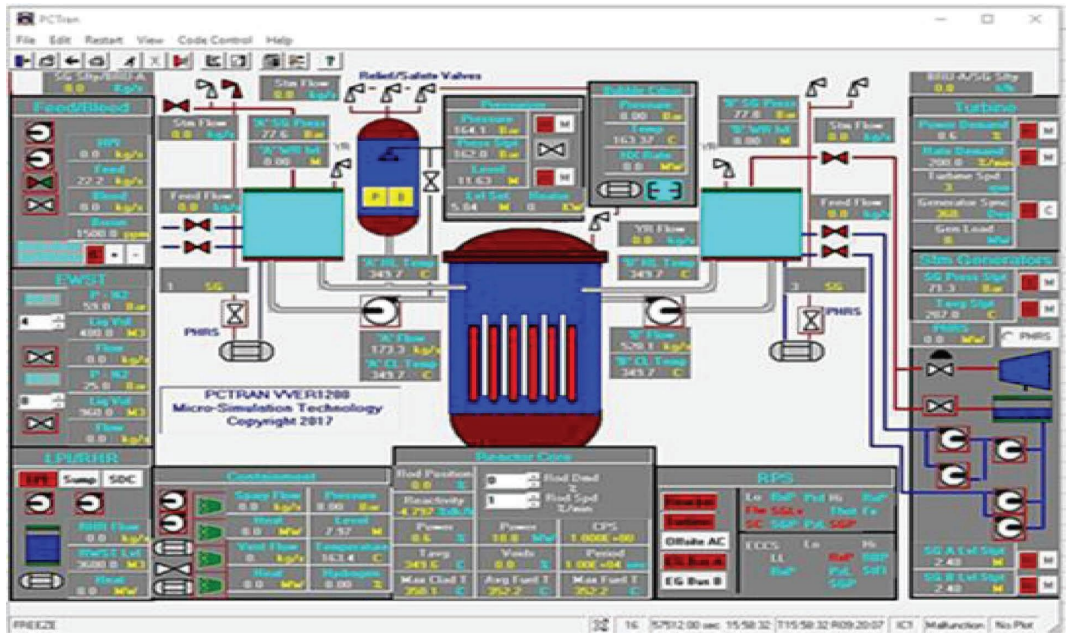

Figure 2: The end of LTSBO simulation main view of PCTRAN.

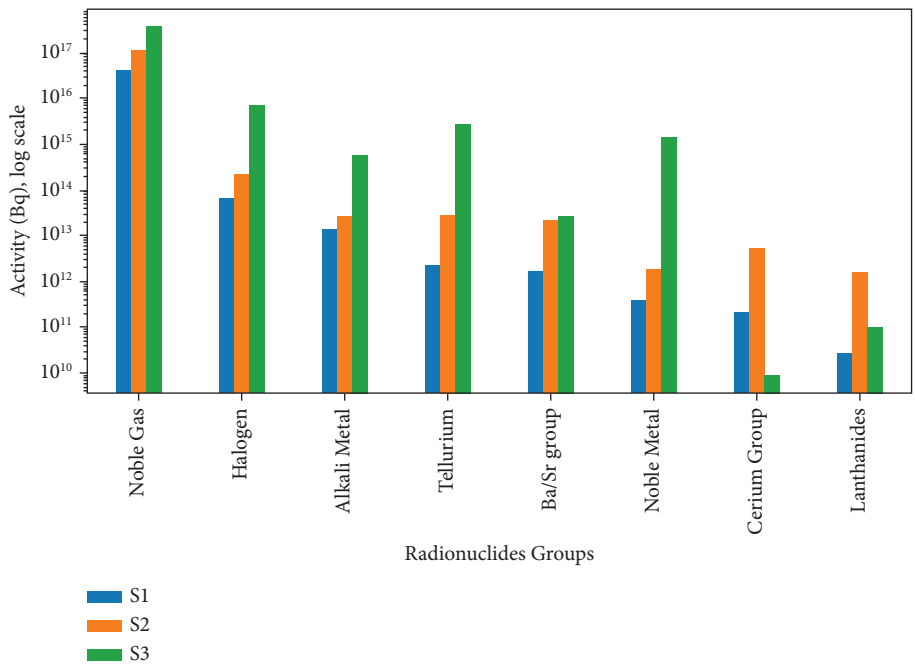

Figure 3: The source term groups activity in Becquerel (Bq) for all scenarios.

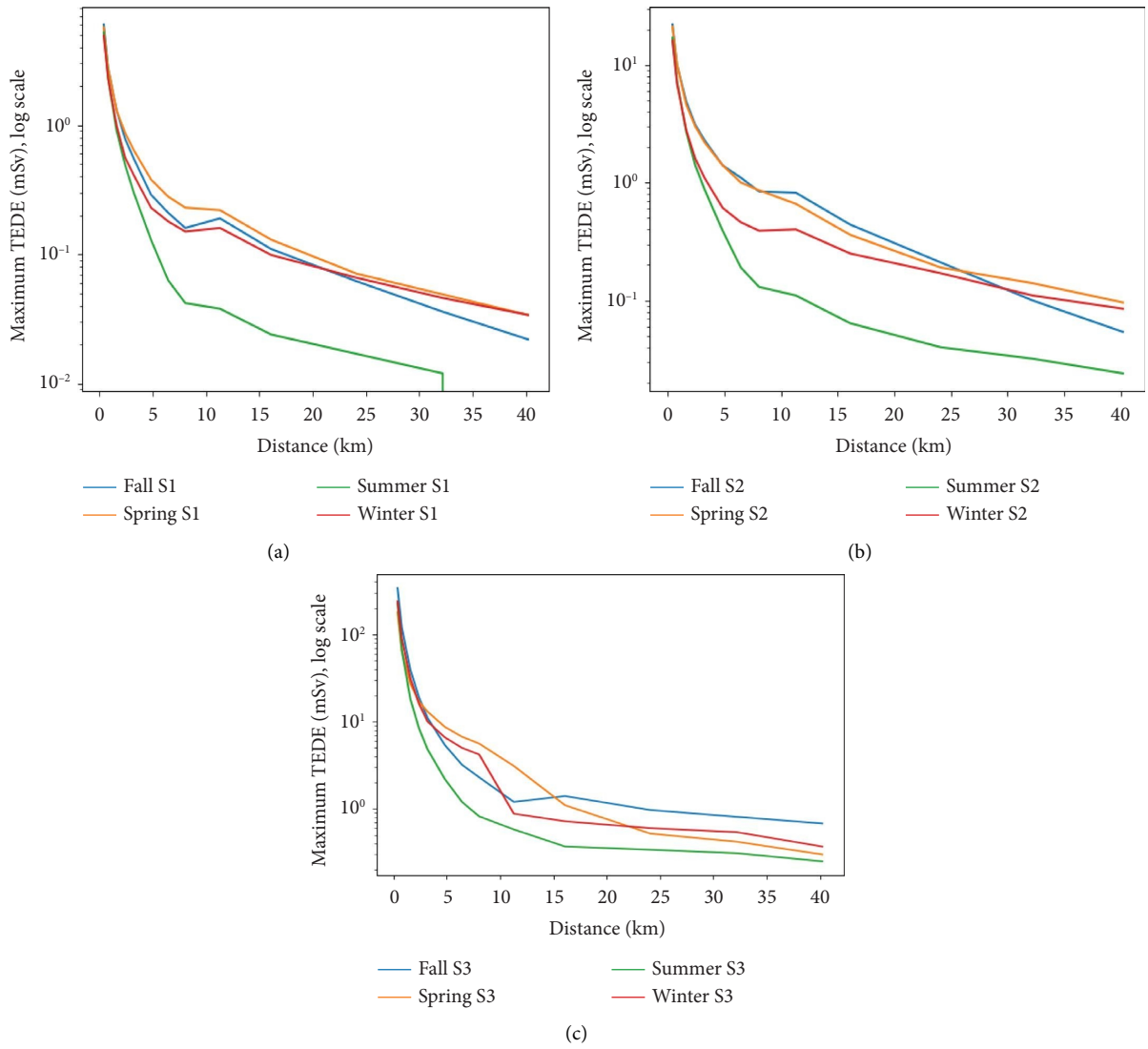

Figure 4: Maximum TEDE distribution corresponding to distance for (a) S1, (b) S2, and (c) S3, respectively, during four seasons.

availability, S1 (a) at 0.4 km from the release point, the radiation exposure was measured as 6 mSv, 5.7 mSv, 5.2 mSv, and 4.9 mSv during fall, spring, summer, and winter, respectively. The radiation exposure decreased as the distance increased, reaching a maximum of only 0.03 mSv at 40 km. The highest values were observed in spring and winter. with the same LOCA but without ECCS availability, S2 (b) at 0.4 km from the release point, radiation exposure peaked at 22 mSv, 21 mSv, 17 mSv, and 16 mSv for fall, spring, summer, and winter, respectively. Notably under S3 scenario (c), radiation exposure levels near the release point were significantly higher, reaching 340 mSv, 180 mSv, 230 mSv, and 240 mSv for fall, spring, summer, and winter, respectively. As distance increased, the radiation exposure decreased, with a maximum value above the limits of 11 mSv during fall, 13 mSv during spring, 4.8 mSv during summer, and 10 mSv during winter at 3.2 km. For all seasons, at 40 km, the values were much lower than the PAGs limits.

4.2.2. Thyroid Committed Dose Equivalent. The highest dose values for thyroid dose (TD) in mSv were also computed within a 40.2 km from the nuclear plant. These findings were visually depicted in Figure 5, with panels (a), (b), and (c) corresponding to scenarios S1, S2, and S3, respectively.

As a worst-case scenario particularly scenario S3 (c) the TD reached $3.8E+03$ mSv, $2.0E+03$ mSv, $2.2E+03$ mSv, and $2.9E+09$ mSv during fall, spring, summer, and winter, respectively, at 0.4 km. As the distance from the release point increased, radiation exposure diminished, but still remained concerning. At 4.8 km, the maximum values exceeded the prescribed limits, with readings of $6.1E+01$ mSv in fall, $9.9E+01$ mSv in spring, and $8.2E+01$ mSv in winter. Furthermore, in the context of scenario S2, a noteworthy observation is that the thyroid dose (TD) surpasses the limits only at a distance of 0.4 km from the release point. Specifically, during fall and spring, the TD was measured at 100 mSv, which is double the prescribed limits. However, during the summer and winter seasons, these values were

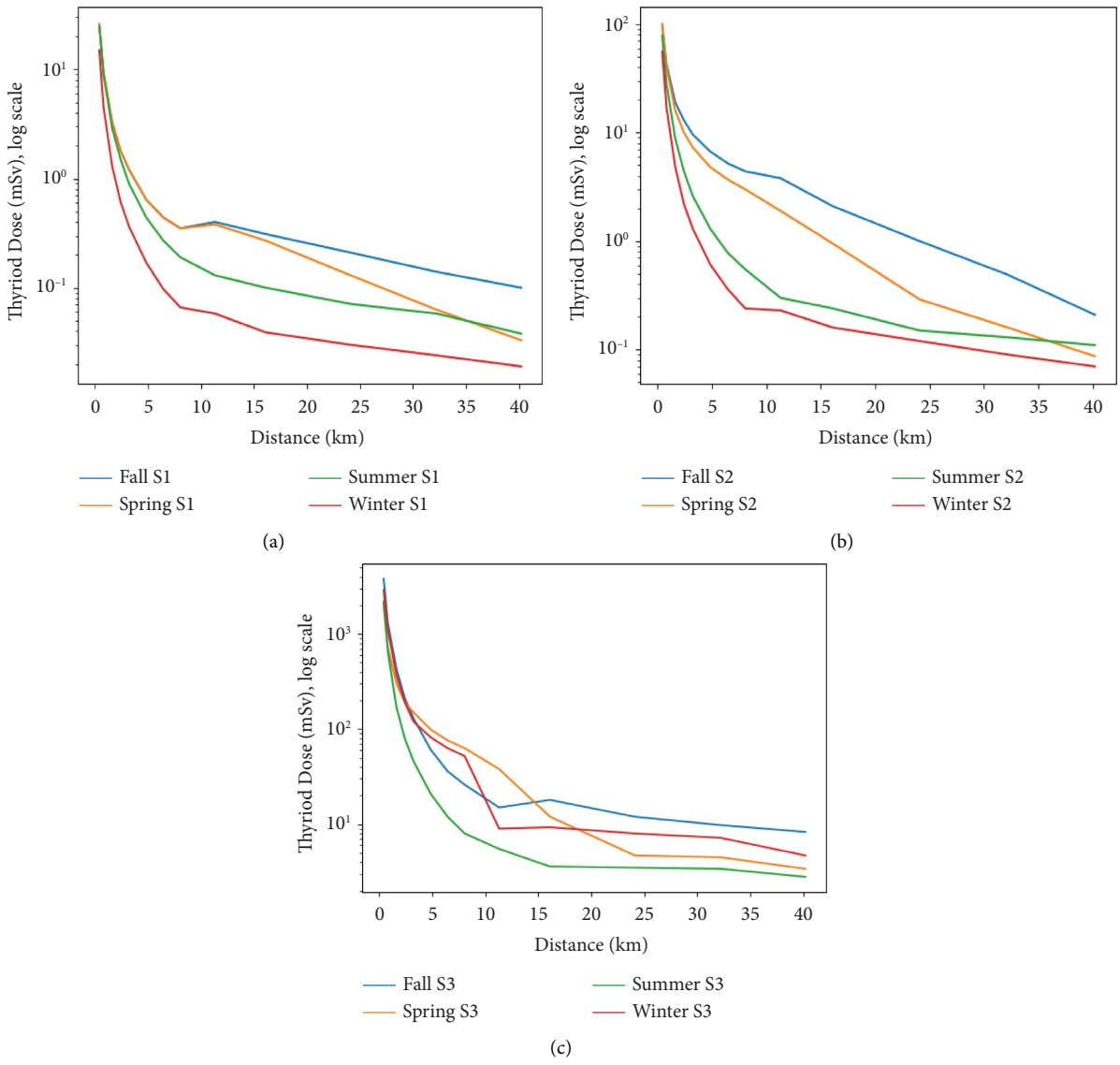

Figure 5: Thyroid dose distribution a long distance for S1 (a), S2 (b), and S3 (c),respectively.

slightly lower at 76 mSv and 56 mSv, respectively. On the contrary, in scenario S1, it is crucial to emphasize that across all seasons, the recorded values were significantly below the limits stipulated by Protective Action Guides (PAGs).

Variations arise from facility-specific factors such as source term, operational conditions, the presence of safety systems affecting release activity, and the implementation of mitigation measures. These results underscore the importance of taking into account precise accident scenarios and the corresponding weather conditions when evaluating the potential impact of radiation.

In the early stage of a severe nuclear incident, critical measures are used to mitigate consequences and manage the crisis effectively. PAGs are pivotal in guiding decisions, ensuring public health and safety. Regulatory authorities develop these PAGs, founded on scientific and technical evaluations [40]. Accurate evaluation of radiation doses from deposited materials, aiding decisions on protective actions and understanding radiological impacts. Table 4 delineates crucial PAG components for early phase of nuclear accidents, along with recommended actions for this study.

These findings highlight that neither the TEDE nor thyroid dose values come close to regulatory limits, as observed in the case of LOCA S1. This indicates that there is no immediate need for concern regarding regulatory thresholds for both workers and the general public. For LOCA S2, it is only beyond a distance of 800 meters from El Dabaa unit 1 that some protective actions might be warranted for workers, in line with the "as low as reasonably achievable" (ALARA) principle following an incident. Importantly, there is no requirement for an emergency plan for the public in this scenario, as they remain safe. However, the Long-Term Station Blackout (LTSBO) scenario (S4) raises the necessity for specific protective measures. This is due to the observation that both TEDE and hyroid dose values remain elevated beyond the established limits within an 11 km and 4.8 km, respectively, after 96 hours.

Table 4: PAGs and suggested protective actions for study accidents scenarios.

PAGs [41]		LTSBO S3		LOCA S2	LOCA S1
Early phase protective actions (4 days)					
TEDE (10–20 mSv)	Thyroid dose (50 mSv)	During fall, spring and winter within population within 3.2 km	(i) During all seasons KI should be distributed to the population within 6.4 km from the site (ii) The distribution should be expanded in spring to 8 km (following footprint of Figure 6 for directions and affected areas)	Applied ALARA to the worker	N/A
Sheltering and evacuation	Administration of prophylactic drugs–KI	Should be go under sheltering and evacuation plan			

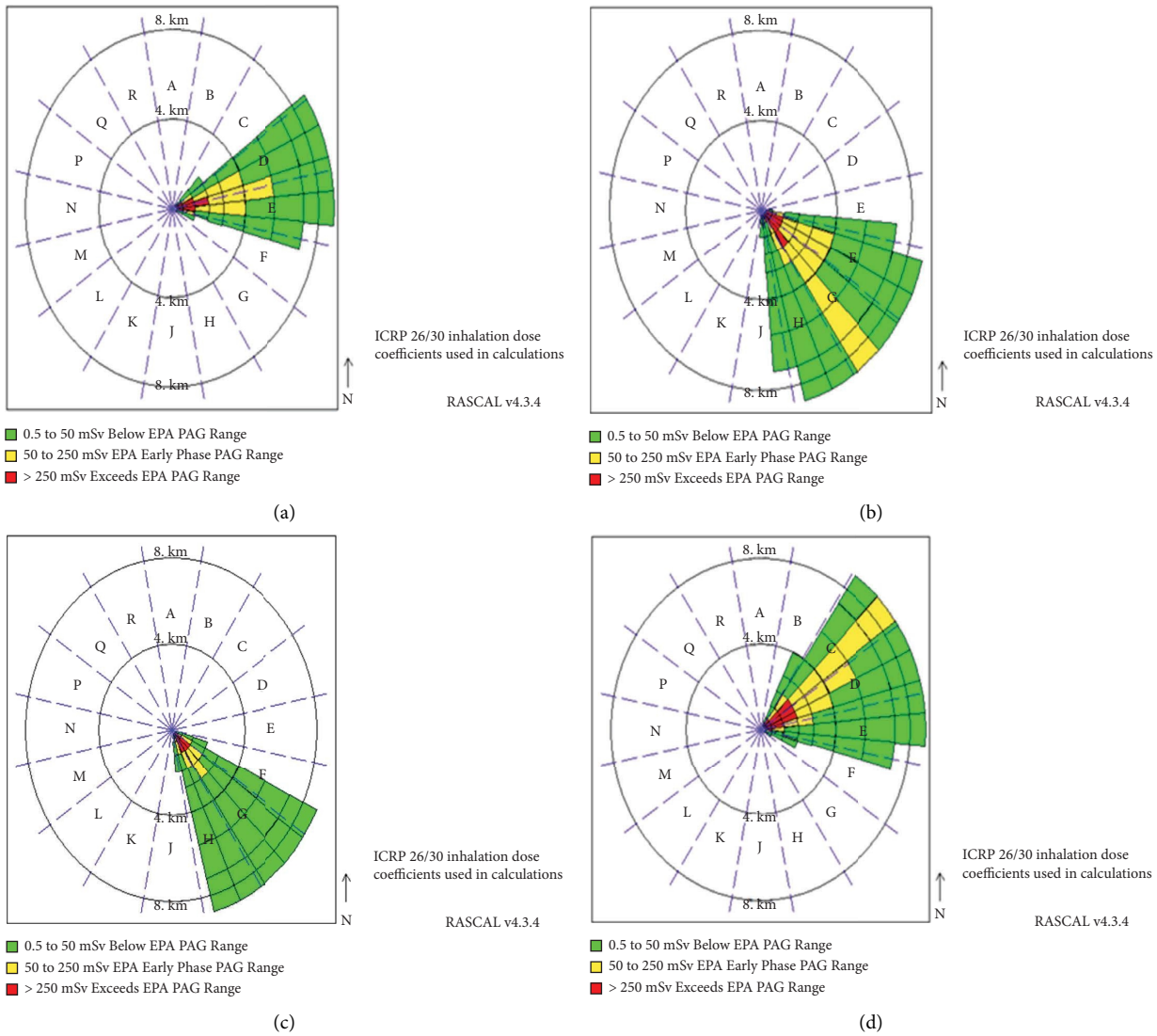

Figure 6: Thyroid footprint for (a) fall, (b) spring, (c) summer, and (d) winter in case of LTSBO S3.

LTSBO emerged as the worst-case scenario in all seasons, surpassing ICRP and PAGs regulation limits [41, 42]. Results in Figure 6 shows that during fall, plume expansion within the early phase range from 70 to 90 degrees covered 3.8 km^2, with the maximum doses $6.1E-02$ Sv at 4.8 km in 80 degrees. During spring, 1.7 km^2 was covered within 110 and 140 degrees where the expansion of the plume dose limits was $6.3E-02$ Sv reaching 8 km. Summer experienced directional patterns between 130 to 140 with 0.2 km^2 above 50 mSv. In 50-degrees direction, the dose reached 8 km with $5.2E-02$ where the dispersion is directed to the sea.

The Food and Drug Administration (FDA) has updated its guidelines for the use of stable iodine, referred to as "KI," as a thyroid-blocking agent in radiological

Table 5: Threshold levels of radioactive exposure to the thyroid gland and the recommended dosages of potassium iodide (KI) for various risk groups [41].

Thyroid dose (mSv)	KI concentration dose (mg)	Risk group age
≥5000	130	Over 40 yr
≥10000	130	Over 18 to 40
≥50	130	Pregnant women
	16–65 (with consideration of different weight)	Infants within 1 month to adolescents with 18 yr

emergencies. These revised recommendations for dosing are informed by thyroid cancer data from the Chernobyl incident and aim to address challenges in effectively administering KI across different exposure levels. Recognizing the logistical complexities involved, the FDA recommends the administration of KI to both children and adults based on the most conservative intervention threshold: projected internal thyroid exposure exceeding 0.05 Sv (50 mSv) for children (Guides & Guidance, 2017). Table 5 shows the potassium iodide (KI) dosages for different risk groups and threshold levels of radioactive exposure to the thyroid gland.

The Long-Term Station Blackout (LTSBO) study offers valuable insights into thyroid dose levels across various seasons, fall, spring, summer, and winter, and considers different directions and distances. These findings, presented in Figure 6 and Table 4, serve as the foundation for establishing the distribution of thyroid-blocking tablets. Aligned with the FDA's guidelines, the study proposes a comprehensive plan for distributing these tablets that is applicable throughout all seasons. The plan outlines varying dosages (ranging from 16 mg to 65 mg) based on weight differences for individuals aged 1 month to 18 years, as well as pregnant women, within specified directions and distances.

5. Conclusion

In conclusion, the study has delved into the critical realm of radiological emergency preparedness by using advanced computational tools to assess potential risks and safety measures at the El Dabaa nuclear site. This study utilized advanced PCTRAN and RASCAL software to evaluate the radiological impacts of hypothetical incidents, including LOCA with and without the availability of ECCS and LTSBO, at the El Dabaa NPP. The integration of advanced tools, including atmospheric dispersion models and high-resolution meteorological databases, is foundational in providing precise projections for radiological events. Over a span of ten years, comprehensive meteorological data were meticulously analyzed to study the dispersion of radioactive substances within a 40-kilometer radius around the El Dabaa NPP throughout all four seasons. This research underscores the significance of early phase dose assessments and comprehensive risk management strategies during radiological emergencies. It is noteworthy that only LTSBO scenario surpassed the radiological exposure limits set by the EPA. During spring, LTSBO recorded a maximum TEDE of 13 mSv at 3.2 kilometers. The expansion of thyroid dose plume ranged from 70 to 90 degrees, covering an area of 3.8 square kilometers. The maximum doses reached $6.1E-02$ Sv at a distance of 4.8 km in the 80-degree direction. During spring, the plume covered 1.7 square kilometers within the range of 110 to 140 degrees, with dose limits extending to $6.3E-02$ Sv up to 8 km. In the summer, directional patterns were observed between 130 to 140 degrees, covering an area of 0.2 square kilometers where doses exceeded 50 mSv. Remarkably, in the 50-degree direction, the dose extended up to 8 kilometers with a value of $5.2E-02$ Sv, and the dispersion was directed towards the sea. Calculated radioactive exposure levels, alongside the recommended use of potassium iodide (KI) for thyroid protection, underscore practical measures for ensuring public health and safety in unforeseen incidents. The study findings provide the foundation for devising a distribution plan for thyroid-blocking tablets. Aligned with FDA guidelines, the study suggests a comprehensive plan applicable across all seasons. This plan specifies varied dosages (ranging from 16 mg to 65 mg) based on weight differences for individuals aged 1 month to 18 years and pregnant women residing within specific directions and distances under worst case scenario. As Egypt embarks on its nuclear journey, this research provides valuable insights for researchers, emergency responders, and policymakers. Enhancing our understanding of radiological risks, safety measures, and potential nuclear incident consequences contributes to public welfare, environmental security, and the efficacy of response planning in emergency scenario.

Data Availability

The data supporting the findings of this study are included within the article.

Conflicts of Interest

The authors declare that they have no conflicts of interest regarding the publication of this article.

Acknowledgments

This research was supported by the 2023 Research Fund of the KEPCO International Nuclear Graduate School (KINGS), the Republic of Korea.

References

[1] Wnn, "Contract signed for El Dabaa turbine islands," 2022, https://www.world-nuclear-news.org/Articles/Contract-signed-for-El-Dabaa-turbine-islands?fbclid=IwAR1KQ3BoYS11EjM61Q__ifBwgqmIUQgAa2fkBFaQjtNCfcOR1QmJGcinhdw.

[2] Y.-H. Cheng, C. Shih, S.-C. Chiang, and T.-L. Weng, "Introducing PCTRAN as an evaluation tool for nuclear power plant emergency responses," *Annals of Nuclear Energy*, vol. 40, no. 1, pp. 122–129, 2012.

[3] A. Fairuz and M. H. Sahadath, "Assessment of the potential total effective dose (TED) and ground deposition (GD) following a hypothetical accident at the proposed Rooppur nuclear power plant," *Applied Radiation and Isotopes*, vol. 158, Article ID 109043, 2020.

[4] A. Abbasi, "Prediction of radioactive materials distribution from a hypothetical accident in Akkuyu NPP," 2023, https://europepmc.org/article/ppr/ppr635980.

[5] G.-S. Choi, J.-M. Lim, K. S. Sunny Lim, K.-H. Kim, and J.-H. Lee, "Characteristics of regional scale atmospheric dispersion around Ki-Jang research reactor using the Lagrangian Gaussian puff dispersion model," *Nuclear Engineering and Technology*, vol. 50, no. 1, pp. 68–79, 2018.

[6] Iaea, *Criteria for Use in Preparedness and Response for a Nuclear or Radiological Emergency*, IAEA Safety Standards Series, Vienna, Austria, 2011.

[7] I. A. Alrammah, "Analysis of nuclear accident scenarios and emergency planning zones for a proposed Advanced Power Reactor 1400 (APR1400)," *Nuclear Engineering and Design*, vol. 407, Article ID 112275, 2023.

[8] C. Fayers, "PC CREAM: a PC package to assess the consequences of radioactive discharges due to normal operations," *IRPA9: 1996 international congress on radiation protection, Proceedings*, vol. 2, 1996.

[9] Y. Rentai, "Atmospheric dispersion of radioactive material in radiological risk assessment and emergency response," *Progress in Nuclear Science and Technology*, vol. 1, pp. 7–13, 2011.

[10] J. Ramsdell, G. Athey, and J. Rishel, *RASCAL 4: Description of Models and Methods. United States Nuclear Regulatory Commission*, office of nuclear security and incident respons, Bethesda, MD, USA, 2012.

[11] J. V. R. S. A. McGuire and G. F. Athey, *RASCAL 3.0.5: Description of Models and Methods (NUREG-1887)*, United States Nuclear Regulatory Commission, Rockville, MD, USA, 2007.

[12] A. Saha, N. Fyza, A. Hossain, and M. R. Sarkar, "Simulation of tube rupture in steam generator and transient analysis of VVER-1200 using PCTRAN," *Energy Procedia*, vol. 160, pp. 162–169, 2019.

[13] C. P. Li-Chi and J. M. Link, "PCTRAN-3: the third generation of personal computer-based plant analyzer for severe accident management," 2004, https://inis.iaea.org/search/search.aspx?orig_q=RN:35095516.

[14] S. Shay, *Egypt and the El-Dabaa Nuclear Plant*, Institute for Policy and Strategy Publications, Herzliya, Israel, 2018, https://bit.ly/3AO8mBQ.

[15] W. F. Bakr, "AKA, assessing the emergency planning zones for the Egyptian nuclear power plant site," *IOSR Journal of Applied Physics*, vol. 10, no. 5, pp. 13-14, 2018.

[16] M. B. Roth and P. Jaramillo, "Going nuclear for climate mitigation: an analysis of the cost effectiveness of preserving existing US nuclear power plants as a carbon avoidance strategy," *Energy*, vol. 131, pp. 67–77, 2017.

[17] A. H. Khan, M. I. Al Imran, N. Fyza, and M. Sarkar, "A numerical study on the transient response of VVER-1200 plant parameters during a large-break loss of coolant accident," *Indian Journal of Science and Technology*, vol. 12, pp. 1–12, 2019.

[18] K. Buesseler, M. Aoyama, and M. Fukasawa, "Impacts of the Fukushima nuclear power plants on marine radioactivity," *Environmental Science and Technology*, vol. 45, no. 23, pp. 9931–9935, 2011.

[19] T. J. Yasunari, A. Stohl, R. S. Hayano, J. F. Burkhart, S. Eckhardt, and T. Yasunari, "Cesium-137 deposition and contamination of Japanese soils due to the Fukushima nuclear accident," *Proceedings of the National Academy of Sciences*, vol. 108, no. 49, pp. 19530–19534, 2011.

[20] Y.-H. Koo, Y.-S. Yang, and K.-W. Song, "Radioactivity release from the Fukushima accident and its consequences: a review," *Progress in Nuclear Energy*, vol. 74, pp. 61–70, 2014.

[21] L. Sihver and N. Yasuda, "Causes and radiological consequences of the Chernobyl and Fukushima nuclear accidents," *Journal of Nuclear Engineering and Radiation Science*, vol. 4, no. 2, 2018.

[22] F. Rocchi, A. Guglielmelli, F. Padoani, and P. Meloni, "Application of RASCAL 4.2 to estimate the Fukushima accident source term," in *Proceedings of the International Conference on Challenges Faced by Technical and Scientific Support Organizations (TSOs) in Enhancing Nuclear Safety and Security*, Brussels, Belgium, October 2014.

[23] S. Omar and M. N. Hasan, "A PCTRAN based analysis on the effect of break size and comparative study between hot and cold leg loss of coolant accidents in VVER 1200 power reactor," *Acta Mechanica Malaysia*, vol. 5, no. 2, pp. 31–34, 2022.

[24] N. Fyza, A. Hossain, and R. Sarkar, "Analysis of the thermal-hydraulic parameters of VVER-1200 due to loss of coolant accident concurrent with loss of offsite power," *Energy Procedia*, vol. 160, pp. 155–161, 2019.

[25] S. Akter, M. S. A. Joarder, M. G. Zakir, A. Hossain, M. A. Razzak, and M. S. Islam, "Comparative analysis of thermal hydraulic parameters of AP-1000 and VVER-1200 nuclear reactor for turbine trip concurrent with anticipated transient without SCRAM (ATWS)," in *Proceedings of the 2021 International Conference on Automation, Control and Mechatronics for Industry 4.0 (ACMI)*, pp. 1–6, IEEE, Rajshahi, Bangladesh, July 2021.

[26] M. M. H. Tanim, M. F. Ali, M. A. Shobug, and S. Abedin, "Analysis of various types of possible fault and consequences in VVER-1200 using PCTRAN," in *Proceedings of the 2020 International Conference for Emerging Technology (INCET)*, pp. 1–4, IEEE, Belgaum, India, June 2020.

[27] A. Abd El-Hameed and J. Kim, "A machine learning-based approach to the prediction of accidental source term," 2021, https://www.academia.edu/84875404/A_Machine_Learning_Based_Approach_to_the_Prediction_of_Accidental_Source_Term.

[28] N. T. Khai and L. D. Cuong, "Assessment of radioactive gaseous effluent released from Ninh Thuan 1 Nuclear power plant under scenario of INES-level 7 Nuclear accident," *Communications Physics*, vol. 25, no. 4, pp. 375–382, 2016.

[29] S. I. Faisal, M. S. Islam, and M. A. Malek Soner, "Prediction of radioactivity releases for a Long-Term Station Blackout event in the VVER-1200 nuclear reactor of Bangladesh," *Nuclear Engineering and Technology*, vol. 55, no. 2, pp. 696–706, 2023.

[30] S. S. Shiuli, M. A. Khaer, M. M. Islam et al., "Assessment of radiological safety and emergency response of VVER-1200

type reactor," *International Journal of Advanced Nuclear Reactor Design and Technology*, vol. 4, no. 2, pp. 70–79, 2022.

[31] A. Sjoreen, G. Athey, C. A. Sakenas, and T. J. McKenna, *Screening Model for Assessing Doses from Radiological Accidents*, Oak Ridge National Lab, Oak Ridge, TN, USA, 1988.

[32] J. Ramsdell Jr., G. Athey, J. Rishel, and T. Hay, *RASCAL 4.3 Technical Supplement (Draft)*, US National Regulatory Commission, Washington, DC, USA, 2013.

[33] U. S. E. P. A. O. O. R. Programs, *Manual of Protective Action Guides and Protective Actions for Nuclear Incidents*, Office of Radiation Programs, US Environmental Protection Agency, Washington, DC, USA, 1989.

[34] W. Simulator, *PCTRAN Generic Pressurized Water Reactor Simulator Exercise Handbook*, INTERNATIONAL ATOMIC ENERGY AGENCY, Vienna, Austria, 2019.

[35] D. Tecdoc, *Considerations On The Application Of The Iaea Safety Requirements For Design Of Nuclear Power Plants*, IAEA, Vienna, Austria, 2014.

[36] Iaea, "Status report 108- VVER-1200 (V-491) (VVER-1200 (V-491))," 2011, https://aris.iaea.org/PDF/VVER-1200(V-491).pdf.

[37] R. Overseas, *The VVER Today: Evolution, Design, Safety*, Rosatom Overseas, Moscou, Russia, 2013.

[38] V. G. Asmolov, I. N. Gusev, V. R. Kazanskiy, V. P. Povarov, and D. B. Statsura, "New generation first-of-the kind unit–VVER-1200 design features," *Nuclear Energy and Technology*, vol. 3, no. 4, pp. 260–269, 2017.

[39] S. Jafarikia and S. Feghhi, "Study of in-containment source term behavior for VVER-1000 under LOCA conditions using the IRBURN code system," *Annals of Nuclear Energy*, vol. 112, pp. 17–29, 2018.

[40] P. Manual, *Protective Action Guides and Planning Guidance for Radiological Incidents*, Draft for Interim Use and Public Comment, Washington, DC, USA, 2013.

[41] P. A. Guides and P. Guidance, "PAG manual," 2017, https://www.epa.gov/sites/default/files/2017-01/documents/epa_pag_manual_final_revisions_01-11-2017_cover_disclaimer_8.pdf.

[42] R. Sievert and G. Failla, "Recommendations of the international commission on radiological protection," *Health Physics*, vol. 2, 1959.